BMC Veterinary Research

RESEARCH

Open Access

Cinnamon nanoemulsion mitigates acetamiprid-induced hepatic and renal toxicity in rats: biochemical, histopathological, immunohistochemical, and molecular docking analysis

Ahmed A. A. Aioub[1*], Sameh A. Abdelnour[2], Ahmed S. Hashem[3], Mohamed Maher[4], Sarah I. Z. Abdel-Wahab[1], Lamya Ahmed Alkeridis[5], Mustafa Shukry[6], Samy M. Sayed[7,8] and Ahmed E. A. Elsobki[1]

Abstract

Acetamiprid (ACDP) is a widely used neonicotinoid insecticide that is popular for its efficacy in controlling fleas in domestic settings and for pets. Our study aims to offer a comprehensive examination of the toxicological impacts of ACDP and the prophylactic effects of cinnamon nanoemulsions (CMNEs) on the pathological, immunohistochemical, and hematological analyses induced by taking ACDP twice a week for 28 days. Forty healthy rats were divided into four groups ($n = 10$) at random; the first group served as control rats; the second received CMNEs (2 mg/Kg body weight); the third group received acetamiprid (ACDP group; 21.7 mg/Kg body weight), and the fourth group was given both ACDP and CMNEs by oral gavage. Following the study period, tissue and blood samples were extracted and prepared for analysis. According to a GC-MS analysis, CMNEs had several bioactive ingredients that protected the liver from oxidative stress by upregulating antioxidant and anti-inflammatory agents. Our findings demonstrated that whereas ACDP treatment considerably boosted white blood cells (WBCs) and lymphocytes, it significantly lowered body weight gain (BWG), red blood cells (RBCs), hemoglobin (Hb), hematocrit (HCT), and platelets (PLT). ACDP notably reduced antioxidant enzyme activities: superoxide dismutase (SOD), glutathione peroxidase (GPx), and catalase (CAT) and elevated hydrogen peroxide and malondialdehyde levels compared with other groups. ACDP remarkably raised alanine aminotransferase (ALT), aspartate amino transaminase (AST), and alkaline phosphatase (ALP) levels.

Moreover, the histopathological and immunohistochemistry assays discovered a severe toxic effect on the liver and kidney following ACDP delivery. Furthermore, cyclooxygenase 2 (COX-2) + immunoexpression was enhanced after treatment with CMNEs. All of the parameters above were returned to nearly normal levels by the coadministration of CMNEs. The molecular docking of cinnamaldehyde with COX-2 also confirmed the protective potential of CMNEs against ACDP toxicity. Our findings highlighted that the coadministration of CMNEs along with ACDP diminished its toxicity by cutting down oxidative stress and enhancing antioxidant capacity, demonstrating the effectiveness of CMNEs in lessening ACDP toxicity.

*Correspondence:
Ahmed A. A. Aioub
a.aioub@zu.edu.eg; ahmedaioub1991@gmail.com
Full list of author information is available at the end of the article

Keywords Acetamiprid, Cinnamon nanoemulsions, Biochemical changes, Histological and immunobiological analysis, In silico analysis

Introduction

Pesticides stand out as one of the most pervasive types of pollutants worldwide but come with significant drawbacks, primarily their toxicity [1]. Poorly executed spraying techniques, whether from misuse, overuse, or intentional abuse, can result in considerable adverse effects on crop production while also posing risks to the environment and human health [2] and inducing potential toxicity to humans [3] as well as non-target organisms [4]. Therefore, long-term exposure can harm human life and interfere with the operation of diverse body organs [5, 6]. Consequently, pesticide side effects have drawn attention from across the world.

Neonicotinoids are a class of insecticides that have recently gained popularity in agricultural pest control [7]. One of the neonicotinoid pesticides, acetamiprid (ACPD), operates on insects' acetylcholine (nACh) receptors and has rapidly gained attraction in the international market [8]. ACPD is water soluble, easily absorbed by plants through their leaves or roots, distributed throughout plant tissues, and prone to leaching into waterways and soil wastes [9]. Therefore, it can accumulate in the human body or non-target organisms [10]. After inhaling ACPD, patients experience headaches, dizziness, nausea, vomiting, and other symptoms [11], and it reaches the liver, kidney, adrenal glands, and thyroid [12]. Various studies have proved that exposure to ACPD induced hepatotoxicity [11, 13], neurotoxicity [14], cytotoxicity, and genotoxicity [15].

Multifarious in vivo and in vitro studies have claimed that ACPD evoked a disproportion between the body's antioxidant defense system and oxidants, generating oxidative stress [15]. In addition to impairing the cellular functioning of diversified organs and degrading cellular macromolecules like proteins and lipids, oxidative stress also lowers antioxidant levels. It heightens lipid peroxidation, DNA damage, and genotoxicity [16]. Oxidative stress production has been discovered to be crucial in liver damage [11] and kidney injury [17] caused by ACMP. Another finding from a recent study was the dysregulation and abnormality in amino acid and fatty acid metabolism, which changed the biochemistry of lipids and may have contributed to the development of oxidative stress in liver tissue [13]. Moreover, the oxidative stress produced by ACPD leads to severe oxidative damage to hepatic cells, which results in hepatic cell death and malfunction. These data indicate that oxidative stress will always play a role in ACMP-induced liver damage.

Cinnamon (*Cinnamomum verum*) is a traditional medicinal herb used to treat diabetes, inflammatory diseases, and cancers [16]. Cinnamaldehyde, cinnamic acid, and other distinct chemicals present in cinnamon, together with essential oils, exhibit a range of biological activities, such as antioxidant [18], anti-inflammatory [19], and antitumor properties [20]. Moreover, cinnamon exhibits hepatoprotective and nephroprotective effects [21]. Furthermore, cinnamon has hepatoprotective activity against alcohol and carbon tetrachloride-induced hepatic injury [22]. Likewise, Sakr et al. [23] pinpointed that cinnamon was protective in kidney injury induced by cypermethrin.

With its vast array of potential applications, nanotechnology has experienced tremendous progress [24]. A type of emulsion known as nanoemulsions has droplet sizes ranging from 20 to 500 nm [25]. Nanoemulsions are employed in various biological applications because of their unique features, such as strong stability and controllable rheology [26]. Some studies have proven that cinnamon was utilized to lessen the toxicity and oxidative stress caused by pesticides in living things [27]. However, no study has been published till now about using cinnamon in CMNEs form as an ameliorating effect against ACPD in rats.

Consequently, we hypothesized that CMNEs might enhance antioxidant capacity and reduce proinflammatory mediators in male rats, thereby counteracting the harmful effects of ACPD-induced toxicity. This study aimed to examine the ameliorative function of CMNEs against the deleterious effects of ACPD on liver and renal tissues, as well as the combined and independent effects of ACPD and CMNEs on body weight growth in test rats. Furthermore, hematological parameters, histopathological alterations, oxidative stress levels, and antioxidant enzyme levels were assessed in both liver and kidney tissues. Additionally, the liver and kidney tissues were subjected to immunohistochemical analysis to evaluate the expression of COX-2 under the influence of ACPD stress. Moreover, molecular docking was performed to investigate the interaction between the primary component of CMNEs and COX-2, with cinnamaldehyde acting as the ligand and COX-2 as the receptor.

Materials and methods

Chemicals and reagents

Acetamiprid (ACPD, 97%) was obtained from Sigma, China. ALT, AST, ALP, SOD, CAT, malondialdehyde

(MDA), hydrogen peroxide (H_2O_2), and GPx kits were obtained from Biodiagnostic Company (Dokki, Giza, Egypt).

Nanoemulsion preparation and characterization

The nanoemulsion (NE) containing Cinnamomum verum essential oil (EO) was synthesized at the Agricultural Research Center in Sakha, Kafr El-Sheikh (coordinates: 66.7613° N, 124.1238° E) using the method outlined by Hamouda et al. Hamouda et al. [28], with slight modifications as described by Hashem et al. Hashem et al. [29]. Briefly, Thickened O/W nanoemulsions were made using Tween 80 (3%, v/v), ethanol (3%, v/v), and C. verum essential oil (14%, v/v of the total coarse emulsion), which accounted for 20% (v/v) of the overall emulsion. After mixing, the oil phase components were stored at 86 °C for one hour. After that, they were combined with 80% water, left for three minutes, and then centrifuged at 10,000 ×g. The cinnamon oil nanoemulsion was kept in dark vials at room temperature until more analysis.

Concerning the characterization of the cinnamon oil nanoemulsion, the dynamic laser light-scattering method (DLS) was utilized to ascertain the droplet size distribution (analysis by volume). Zeta potential, viscosity, conductivity, and polydispersity index (PDI) were investigated by photon correlation spectroscopy (Malvern Zetasizer Nano-zs90, Malvern Instruments Ltd., Enigma Business Park, Grovewood Road, Malvern, Worcestershire, WR14 1XZ, UK). The morphological examination of the cinnamon oil nanoemulsion was performed by adopting a JEOL JEM-2100 transmission electron microscope (TEM) operating at 120 kV. The samples were placed on copper grids and allowed to dry at room temperature. Then, the TEM was inspected without staining.

Gas chromatography-mass spectrometry (GC–MS) analysis

The phytoconstituents of CMNEs were analyzed by a TRACE™ 1310 gas chromatography equipped with Fisher Trace ISQ mass spectrometer (GC-MS) column (SLB™-5ms 30 m × 0.25 mm × 0.25 µm, Sigma-Aldrich, St. Louis, MO, USA). A helium (purity 6.0, Westfalen AG, Münster, Germany) carrier gas flow rate of 1.5 mL min^{-1} was utilized with a sample injection volume of 1 µL and a split of 1:5 at an injection temperature of 250 °C. Regarding GC settings, the oven program was started at 40 °C for 1 min and increased at 3 K min^{-1} to 60 °C and then at 30 K min^{-1} until 280 °C was reached; the final temperature was kept constant for 8 min [30]. Conversely, the MS operating settings were 250 ∘C for the injector and MS transfer line, 250 ∘C for the ion source, 70 eV for the ionization energy, and a mass scan range of 50–500 amu for the complete ion scan mode (scan time: 0.2 s) [31]. The identification of compounds in both samples involved a comparison of their linear retention indices (RI), retention times (RT), and mass spectra with those obtained from authentic samples (gained from the Sigma-Aldrich Group) and/or the NIST/NBS, Wiley libraries, and relevant literature. Subsequently, individual compounds in both samples were determined by analyzing the peak area on the GC chromatogram [32].

Animal and experimental design

Forty adult Sprague Dawley rats, aged between 13 and 15 weeks and weighing an average of 160 ± 20 g, were sourced from the Laboratory Animal Housing Unit of the Faculty of Veterinary Medicine at Zagazig University in Egypt. These rats were housed in stainless-steel cages under a 12-hour light/dark cycle in a well-ventilated room, ensuring optimal conditions for their well-being. Throughout the study, the rats had ad libitum access to food and water. Animal care and experimental procedures complied with protocols approved by the Zagazig University of Egypt's Faculty of Agriculture Committee (ZU-IACUC/2/F/132/2023), ensuring ethical standards and regulatory requirements were met.

Before the tests began, the experimental animals spent a week becoming used to the lab environment. Forty rats were divided into four experimental groups at random (10 rats /group); Group I, the control group, was administered orally daily with normal saline; Group II received CMNEs orally daily (2 mg/kg bwt) only [33]; Group III was given ACPD orally twice a week at a dosage of 1/10 LD_{50} (21.7 mg/kg bwt) [11]; Group IV received CMNEs after 30 min of ACPD administration orally. z. Rats were examined, and any toxicity-related clinical symptoms were recorded daily. The body weight gain was calculated using the formula: weight gain = [(final body weight − initial body weight)/initial body weight] ×100.

Sampling

The animals were weighed the night after their 28-day treatment period and then starved. Animals had a fasting period of about 12 to 18 h before anesthesia. The experimental animals were anesthetized by isoflurane inhalation (Anesthesia was initiated by placing the rats inside an anesthesia induction chamber (measuring 25 × 25 × 14 cm) where they were exposed to 4% isoflurane (Forane; Abbott Japan Co., Ltd., Tokyo, Japan) following [34] and decapitated to obtain blood samples. The samples were collected in tubes using 10% EDTA as an anticoagulant for hematological analysis. A portion of the blood samples was stored in tubes and given 30 min to coagulate at room temperature, then centrifuged at 3,000 rpm for 20 min. After that, the serum was kept at -20 °C for additional testing (liver enzymes and kidney function markers). Subsequently, the kidney and liver tissues were

collected, and part was homogenized at a 10% (w/v) concentration in potassium phosphate buffer (pH 7.4) using a tissue homogenizer. Following homogenization, the mixture was centrifuged at 3000 g for 10 min at 4 °C. The resultant supernatant was then stored at -20 °C; another part was used for histological and immunohistopathological analyses; the livers and kidneys were removed, saline-washed, and preserved in neutral buffered formalin (10%).

Hematological parameters

The obtained blood samples were examined to ascertain the erythrogram and leukogram profiles, among other hematological characteristics. The erythrogram profile involving (RBC, 10^{12}/L), (Hb, g/L), (HCT, %), mean corpuscular volume (MCV, fL), mean corpuscular hemoglobin (MCH, pg), mean corpuscular hemoglobin concentrations (MCHC, g/dL), (PLT, 10^9/L), mean cell volume (MCV, fL), and the leukogram prole such as (WBC, 10^9/L), lymphocyte percentage, and complete blood counts were estimated via an automated blood cell analyzer (Hemascreen18, Hospitex Diagnostics, Sesto Fiorentino, Italy).

Antioxidant profile

SOD activity was measured using a kit SOD (cat.no. SD 2521) from Biodiagnostic, Cairo, Egypt, and a technique by Nishikimi et al. [35] at 440 nm. CAT activity was measured by Aebi [36] using a kit (cat. no. CA-2517) obtained from Biodiagnostic, Cairo, Egypt, and expressed in units per gram of tissue (U/g) at 510 nm. GPx activity was evaluated using spectrophotometry by a prior investigation by Paglia and Valentine [37]. GPx activity was determined by oxidizing NADPH and GSH with glutathione reductase, detecting the drop in absorbance at 340 nm, and expressing the result in units/mg protein using GPX (cat. no. 2524, Biodiagnostic). Protein levels in kidney homogenates were quantified using the method outlined by Lowry et al. [38] with bovine serum albumin serving as the standard. see the supplementary file.

Oxidative stress measurements

The MDA was expressed as nmol/mg protein and measured at 532 nm using a kit from Biodiagnostic (cat. no. MD-2529), Cairo, Egypt. The kit was developed Ohkawa et al. [39]. H_2O_2 was measured at 610 nm using the methodology proposed by Pick and Keisari [40] utilizing a kit (cat no. MBS841818; MyBioSource, San Diego, USA).

Liver and kidney function

According to earlier research by Reitman and Frankel [41], The measurement of serum concentrations of alanine aminotransferase (ALT) and aspartate aminotransferase (AST) was evaluated calorimetrically using kits (cat. no. AT-1034; Bio-diagnostic). Meanwhile, the levels of ALP were estimated following the methodology of Ellis et al. [42]. Reagent kits from Biomed Diagnostics (Egypt) were utilized to determine serum creatinine, urea, and uric acid levels.

Histopathological examination

The liver and kidney samples were cleaned with xylene, embedded in paraffin, and stored in a 10% formalin solution using an automated tissue processor. After that, 5 µm thick slices were created using a rotating microtome and stained with hematoxylin and eosin [43]. Subsequently, five slices of each test rat's liver and kidney that had been stained were examined under a microscope at different magnifications to evaluate qualitative histological variations and perform histomorphometric analysis. For each investigated organ, the histomorphological alterations in five fields per section were used to grade the histopathological abnormalities in the hepatic and renal tissues. ImageJ was used to quantify changes observed under a microscope before statistical analysis initially.

Immunohistochemical study

To perform immunohistochemical analysis, the avidin-biotin-peroxidase complex procedure, as outlined by Hsu et al. [44], was used to stain COX-2 antigens in the hepatic and renal tissues using rabbit monoclonal anti-COX-2 antibody (ab15191) (Abcam, United Kingdom) and 3,30-diaminobenzidine chromogen (DAB). In addition, To confirm whether the IHC analysis was selective and could eliminate nonspecific responses and false-positive results, the negative controls were treated with phosphate buffer saline rather than primary antibodies [45]. The DAB density did not correlate with the epitope concentration, and the majority of hepatic or renal cells were immune-positive to a variable degree for both indicators. Thus, the fractions of DAB brown spots to the total image regions were calculated to get a quantitative evaluation of the COX-2 immunodepression. Five fixed-size microscopic photographs of organisms or animals were taken using the open-source ImageJ program version 1.41 at the same magnification (×40) and exposure time.

Target proteins and docking studies

The Protein Data Bank (PDB) website was operated to obtain the crystal structures of COX-2 (PDB ID: 6COX). According to GC-MS analysis, cinnamaldehyde was the highest concentration in the CMNEs. Cinnamaldehyde was selected as the ligand of COX-2 protein modeling. Then, cinnamaldehyde was acquired from PubChem and ChemSpider databases and was prepared

by Molecular Operating Environment (MOE) 2014.13 software (Chemical Computing Group Inc, Montreal, Quebec, Canada) [46]. The ligands were decreased by using the CHARMM 99 force field before initiating the docking process. Ramachandran's plot (PROCHECK analysis) was used to evaluate and validate these models. After that, bonds were added, duplicates were eliminated, and three-dimensional (3D) structures were built. After all default parameters were set and the least energy structures were obtained, the ligands were made flexible and manually inserted into the catalytic site cavity of the enzyme model. The binding energy was examined using a full-force field, and the ligand and protein's affinity was evaluated using scoring systems that produced free-binding interaction energies based on molecular force field terms. The optimal ligand interaction was examined and assessed following docking using scoring methods and root-mean-square deviation (RMSD) calculations [47].

Statistical analysis

GraphPad Prism program v.8 (GraphPad Software Inc., La Jolla, CA, United States) was used for data analysis. For multiple comparisons between the groups, we ran a one-way analysis of variance and then handled Tukey's post-hoc test; a statistically significant difference was defined as $p < 0.05$.

Results

Characterization of nanoemulsion

The preparation of *C. verum* EO nanoemulsion involved high-pressure homogenization, resulting in a mean droplet size ranging from 100 nm to 200 nm (expressed as z-diameter), with the majority being 157 nm in size (Fig. 1A). The polydispersity index, which typically ranged between 0.23 and 0.25, reflected a highly uniform distribution of droplet sizes with minimal variation (Fig. 1B). Furthermore, zeta potential (mV), conductivity (mS/cm), and viscosity (cP) of *C. verum* EO-based NE were as follows: -24.2 ± 4.39, 0.028, and 0.887, respectively. Moreover, TEM showed that the particle size ranged from 22 to 37 nm and the droplets were spherical (Fig. 1C).

Identification of CMNEs by GC–MS

The GC-MS chromatogram of CMNEs recorded 32 volatile organic compounds (VOCs). According to their retention duration, peak area, height, molecular weight, molecular formula, and mass spectrum records of the known compounds kept by the National Institute of Standards and Technology (NIST) library, each compound identified the phytocompounds (Table 1). The main components of CMNEs are cinnamaldehyde (37.27%), benzyl alcohol (17.59%), bicyclo[2.2.1] heptan-2-one,1,7,7-trimethyl-(1 S) (8.83%), benzene ethanol (8.54%), and trans-13-octadecenoic acid, methyl ester (7.71%).

Changes in body weight gain

According to Fig. 2, ACDP exposure significantly lowered body weight gain (BWG) ($p < 0.05$) concerning the other treated groups. Control and CMNEs groups had similar weight gains, considerably higher than the ACDP group, which had the most minor gain; the CMNPs + ACDP group showed improved weight gain compared to ACDP alone but did not reach the levels of the control or CMNEs groups, suggesting some mitigation by CMNPs of ACDP's adverse effects on weight.

Hematological parameters changes by ACDP and CMNEs

Table 2 exhibited a substantial decrease in RBCs, HCT PLT, and Hb in the animals exposed to ACDP alone or co-administrated with CMNEs compared to the control and CMNEs groups. ($p < 0.05$). On the other hand, rats that received ACDP alone or with CMNEs displayed considerably higher WBC and lymphocyte levels than the control group ($p < 0.05$). Still, the CMNPs + ACDP showed a significant decrease in the total leukocytic count, accompanied by nonsignificant reductions in the lymphocytes of the ACDP-treated rats. In general, the control and CMNEs groups demonstrated improved hematological parameters.

Biochemical evaluation

Figure 3I and II depicted statistically noteworthy variations between the levels of oxidative stress biomarkers (MDA and H_2O_2) and antioxidant enzymes (SOD, CAT, and GPx) in the hepatic, renal, and serum of treated and controlled rats. The ACDP-treated rats displayed significantly decreased SOD, CAT, and GPx activity in contrast to the dramatically increased MDA and H_2O_2 levels. In the CMNEs + ACDP-treated rat, the GPx, SOD, and CAT levels were lessened, but MDA and H_2O_2 were elevated compared to the control.

Hepatic and renal function biomarkers

ALP, AST, and ALT activity levels in addition to urea, uric acid, and creatinine in ACDP-treated rats, were noticeably higher than in control ($p < 0.05$). Additionally, rats treated with ACDP + CMNEs showed notably reduced levels of ALT, ALP, AST, urea, uric acid, and creatinine activity than those in the control and ACDP-only groups ($p < 0.05$) (Fig. 4).

Histopathological findings

All the experimental groups underwent histopathological examination of the liver and kidney tissues. The central

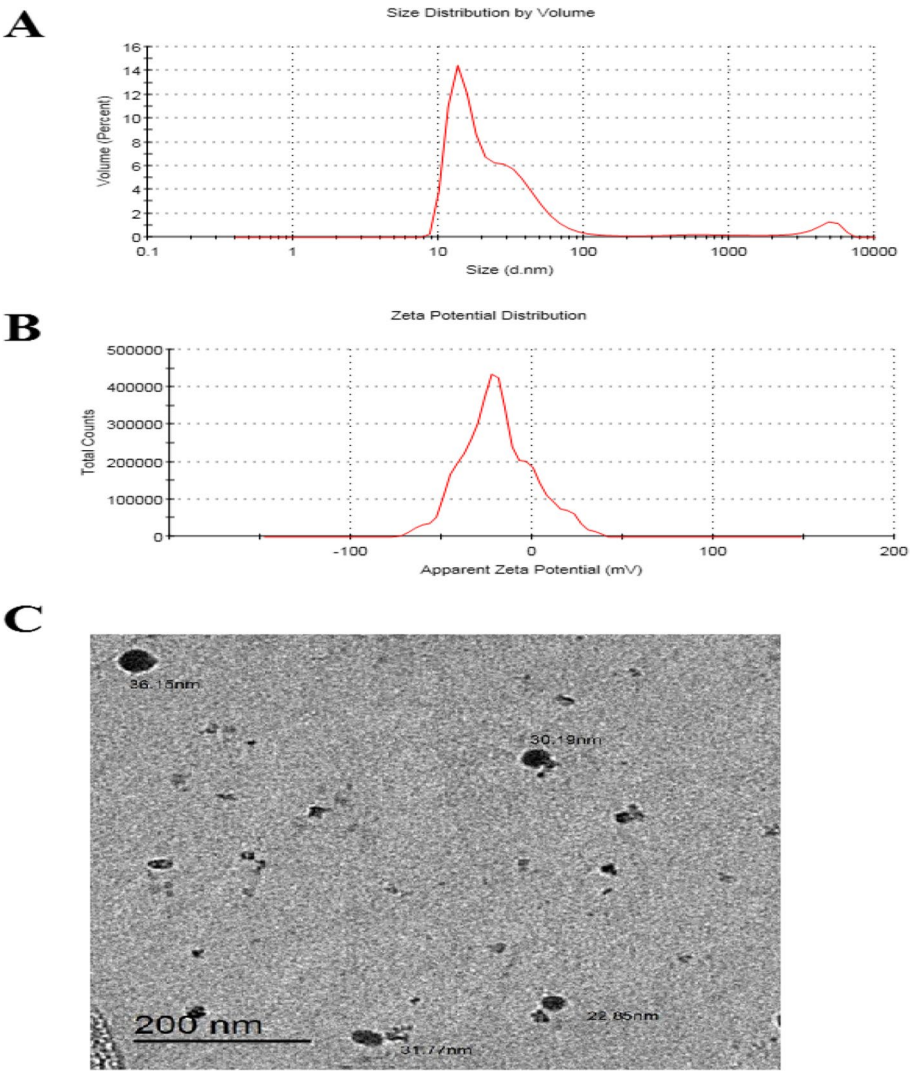

Fig. 1 Characterization of cinnamon oil nanoemulsion. **A** Particle size distribution observed in Dynamic Light Scattering (DLS) instrument, (**B**) Surface net negative charge by Zeta potential, and (**C**) TEM image observe morphology of spherical nanoemulsion

vein and hepatic parenchyma of the livers of both control and CMNEs-treated rats were histologically normal (Fig. 5a, b, Table S1). However, those of the ACPD-treated rats exhibited severe degenerated and necrotic hepatocytes with congested hepatic blood vessels (Fig. 5c, Table S1). The livers of the ACPD + CMNEs-treated rats demonstrated normal hepatic cords with degenerative changes within some hepatocytes (Fig. 5d, Table S1). The kidney tissues of the control and CMNEs-treated rats reflected normal architectures of the glomerular and surrounding tubules of the kidney (Fig. 6a, b, Table S1). ACPD-treated rats exhibited notable characteristics, entailing severe congestion of renal blood vessels (Fig. 6c, Table S1), dilatation of the majority of tubules (Fig. 6d, Table S1), perivascular infiltration of round cells (Fig. 6e, Table S1), and significant hydropic degeneration, necrosis of tubular epithelium, and atrophy of certain glomerular tufts (Fig. 6f, Table S1). In ACPD + CMNEs-treated rats, the kidney revealed normal renal tubules and glomerular structures with some degenerative changes in the renal epithelium (Fig. 6g, Table S1).

Detection of the COX-2

IHC was utilized to identify the location of COX-2 antigens in the rat liver and kidney tissues in all tested groups. Negative COX-2 staining was visible in the tissues of the control and CMNEs-treated rats (Figs. 7 and 8, b). In Fig. 6c, a diffuse immunoexpression of COX-2 antigen is depicted, unveiling widespread positive cytoplasmic staining (golden brown color) in the liver of

Table 1 GC-MS spectral analysis of cinnamon nanoemulsion (CMNEs)

No.	RT[a]	Conc. (%)	Compound	Molecular formula
1	5.23	17.59	Benzyl alcohol	C_7H_8O
2	6.05	0.17	2-Naphthol,1,2,3,4,4a,5,6,7-octahydro-4a-methyl	$C_{11}H_{18}O$
3	6.36	0.17	9,12,15-OCTADECATRIENOIC ACID, METHYL ESTER	$C_{19}H_{32}O_2$
4	6.80	8.54	BENZENEETHANOL	$C_8H_{10}O$
5	7.37	8.83	Bicyclo[2.2.1]heptan-2-one,1,7,7-trimethyl-, (1 S)-	$C_{10}H_{16}O$
6	8.88	0.51	Estragole	$C_{10}H_{12}O$
7	10.27	37.27	Cinnamaldehyde, (E)-	C_9H_8O
8	10.98	0.38	Anethole	$C_{10}H_{12}O$
9	12.69	0.36	Phenol, 2-methoxy-4-(1-propenyl)-	$C_{10}H_{12}O_2$
10	13.19	1.59	2-PROPENOIC ACID, 3-PHENYL-,METHYL ESTER	$C_{10}H_{10}O_2$
11	15.10	0.55	cis-à-Bergamotene	$C_{15}H_{24}$
12	16.79	0.25	á-copaene	$C_{15}H_{24}$
13	19.52	0.50	tau.-Cadinol	C15H26O
14	21.52	0.30	Benzene, [[(1-ethenyl-1,5-dimethyl-4-hexenyl) oxy]methyl]-	$C_{17}H_{24}O$
15	23.96	0.61	2,6,10,14-Hexadecatetraenoic acid, 3,7,11,15-tetramethyl-, methyl ester, (E, E,E)-	$C_{21}H_{34}O_2$
16	24.20	0.23	Ethanol, 2-(9-octadecenyloxy)-, (Z)-	$C_{20}H_{40}O_2$
17	25.19	0.23	1-(2-NITROCYCLOPENTYL)-3-PHENYL-2-PROPEN-1-OL	$C_{14}H_{17}NO_3$
18	25.66	0.40	HEXADECANOIC ACID, METHYL ESTER	$C_{17}H_{34}O_2$
19	26.44	1.06	HEXADECANOIC ACID	$C_{16}H_{32}O_2$
21	28.24	0.29	Bicyclo[3.1.1]hept-3-ene-spiro-2,4'-(1',3'-dioxane), 7,7-dimethyl	$C_{12}H_{18}O_2$
22	28.67	4.22	Methyl 9-cis,11-trans-octadecadienoate	$C_{19}H_{34}O_2$
23	28.85	7.71	trans-13-Octadecenoic acid, methyl ester	$C_{19}H_{36}O_2$
24	29.41	1.00	Methyl stearate	$C_{19}H_{38}O_2$
25	29.60	1.19	[5,9-Dimethyl-1-(3-phenyl-oxiran-2-y l)-deca-4,8-dienylidene]-(2-phenyl-aziridin-1-yl)-amine	$C_{28}H_{34}N_2O$
26	30.81	0.31	RETINOL	$C_{19}H_{30}O_2$
27	35.84	2.01	Diisooctyl phthalate	$C_{24}H_{38}O_4$
28	41.03	0.18	4 H-1-BENZOPYRAN-4-ONE, 2-(3,4-DIMETHOXYPHENYL)-3,5- IHYDROXY-7-METHOXY	$C_{18}H_{16}O_7$
29	42.00	0.22	Ethyl iso-allocholate	$C_{26}H_{44}O_5$
30	42.32	0.70	9,12-OCTADECADIENOIC ACID (Z,Z)-,2,3-BIS[(TRIMETHYLSILYL)OXY]PROPYL ESTER	$C_{27}H_{54}O_4Si_2$
31	43.08	1.67	DOTRIACONTANE	$C_{32}H_{66}$
32	44.25	0.19	1-Heptatriacotanol	$C_{37}H_{76}O$
33	44.76	0.76	Cyclobarbital	$C_{12}H_{16}N_2O_3$

[a] *RT* Retention time

ACPD-treated rats. Conversely, a few immunostained cells by anti-COX-2 in ACDP + CMNEs treated rats were delineated in Fig. 8d. In kidneys, large numbers of immunoexpressed cells with anti-COX-2 in ACDP-treated rats were illustrated as a diffuse positive cytoplasmic expression (golden brown) of COX-2 (Fig. 8c). Contrarily, the kidneys of rats given ACDP + CMNEs treatment displayed only a small number of anti-COX-2 immunostained cells (Fig. 8d). The % area of cox-2 was presented in Fig. 9.

Molecular docking assay

By noticing the binding affinity between the main components of CMNEs (cinnamaldehyde) and COX-2, the molecular docking experiment validates the findings of immunohistochemistry, which unveil that CMNEs protect the liver and kidney tissues from the damaging effects of acetamiprid. The docking scores of interactions between cinnamaldehyde and COX-2 as ligands were delineated in Fig. 10. The docking analysis demonstrated that the investigated cinnamaldehyde had a low docking energy (-16.62 kcal/mol) and a high affinity for the active sites (target enzyme). Cinnamaldehyde as a ligand deeply enters COX-2's hydrophobic pocket (1.01 Å) through two H-pi bonds with Arg 106 and Lys 68, surrounded by the residues Glu 510, Ser 105, Val 74, Tyr 101, and Pro 69.

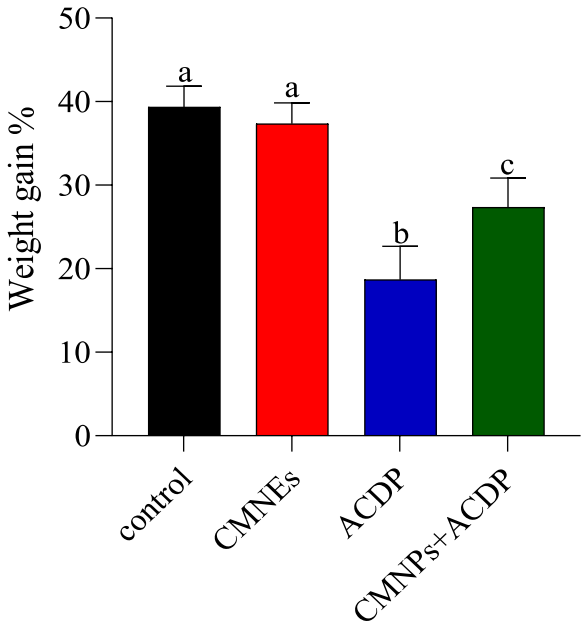

Fig. 2 Effect of cinnamon nanoemulsion (CMNEs; G II) and acetamiprid (ACPD; G III) alone and together (G IV) for 28 days on rat's body weight gain (%) compared with control (G I). The different letters represent the statistically significant differences at ($p < 0.05$) for comparison between all groups, followed by Tukey's post hoc test

Discussion

Pesticides are persistent and shared in the environment, and they pose a risk to people and animals alike, damaging the ecosystem. They can also bioaccumulate and disrupt the food chain [48]. Nanoemulsions, which range in size from 20 to 500 nm, are sometimes called miniemulsions, submicron emulsions, or ultrafine emulsions [49]. There are three different kinds of nanoemulsions combining oil in water (O/W), and water in oil (W/O) [50]. Previous studies proved that nanoemulsion also exhibited anti-inflammatory and antidiabetic properties and potent biological effects against germs and fungi [26]. The *C. verum* EO-based NE exposed a conductivity value, pointing out the presence of slightly conductive ions, which could avoid the polarization of the electrode and boost its stability and nondeteriorating [51].

Moreover, due to the extreme negativity of the zeta potential (-24.2 ± 4.39), there was a significant level of stability [52]. The PDI value (0.24) indicated that the nanoemulsion had good physical stability because the Ostwald ripening was minimized [53], with low viscosity, which might be caused by the low oil content that delayed instability processes and produced oil droplets with a more uniform particle size [54]. Based on TEM evaluation, the droplets were spherical, and the particle size ranged from 22 to 37 nm, consistent with observations of dynamic light scattering. On the other hand, TEM was also employed due to the limitations of DLS's capacity to analyze the nanoparticle structure in detail.

GC-MS is an excellent tool for studying the VOCs from spices and aromatic plants, even at trace levels [55]. Our results from the GC/MS study demonstrated that the extract was enhanced by various bioactive substances that could function as antioxidants, anti-inflammatory substances, and free radical scavengers [56]. Cinnamaldehyde is the highest concentration in the CMNEs. Our data is consistent with research by Wang et al. [56], reporting that cinnamon analysis produced cinnamaldehyde levels ranging from 0.023 to 0.29% w/w. Moreover, The main ingredient in cinnamon oil is cinnamaldehyde [57].

Furthermore, the concentration of cinnamaldehyde in cinnamon oil reached 12.01% [58]. These compositional changes could result from varied environmental (climatic, geographical, or seasonal) and genetic variations. In addition, The content of essential oils varies depending on several variables, including plant sections, the time of year, the extraction process, and the plants' nutritional state [59].

Indefinite environmental pollutants have diverse detrimental health effects on people and animals, especially in poor nations [60]. ACDP-treated rats had significantly lower BWG than the control group. This can be

Table 2 Hematological parameters and blood indices values of control and experimental rat

Parameters	Control	CMNEs	ACDP	CMNPs + ACDP	*P*-value
RBCs (10^{12}/L)	2.60^{a}	2.39^{b}	1.91^{c}	1.94^{c}	0.0002
Platelet (PLT) (10^{9}/L)	77.67^{a}	81.86^{a}	50.33^{b}	48.14^{b}	0.0003
Hemoglobin (Hb) (g/L)	8.71^{a}	8.62^{a}	6.80^{b}	6.98^{b}	0.0002
Hematocrit (HCT) %	36.12^{a}	35.09^{a}	29.97^{b}	29.86^{b}	0.0001
WBCs (10^{9}/L)	6.97^{c}	6.88^{c}	10.73^{a}	8.65^{b}	0.0002
Lymphocytes (%)	78.24^{b}	78.70^{b}	81.95^{a}	81.38^{a}	0.0124

Different letters represent significant differences (Tukey's posthoc test significant difference test among all groups)

RBC red blood cell, *WBC* white blood cell

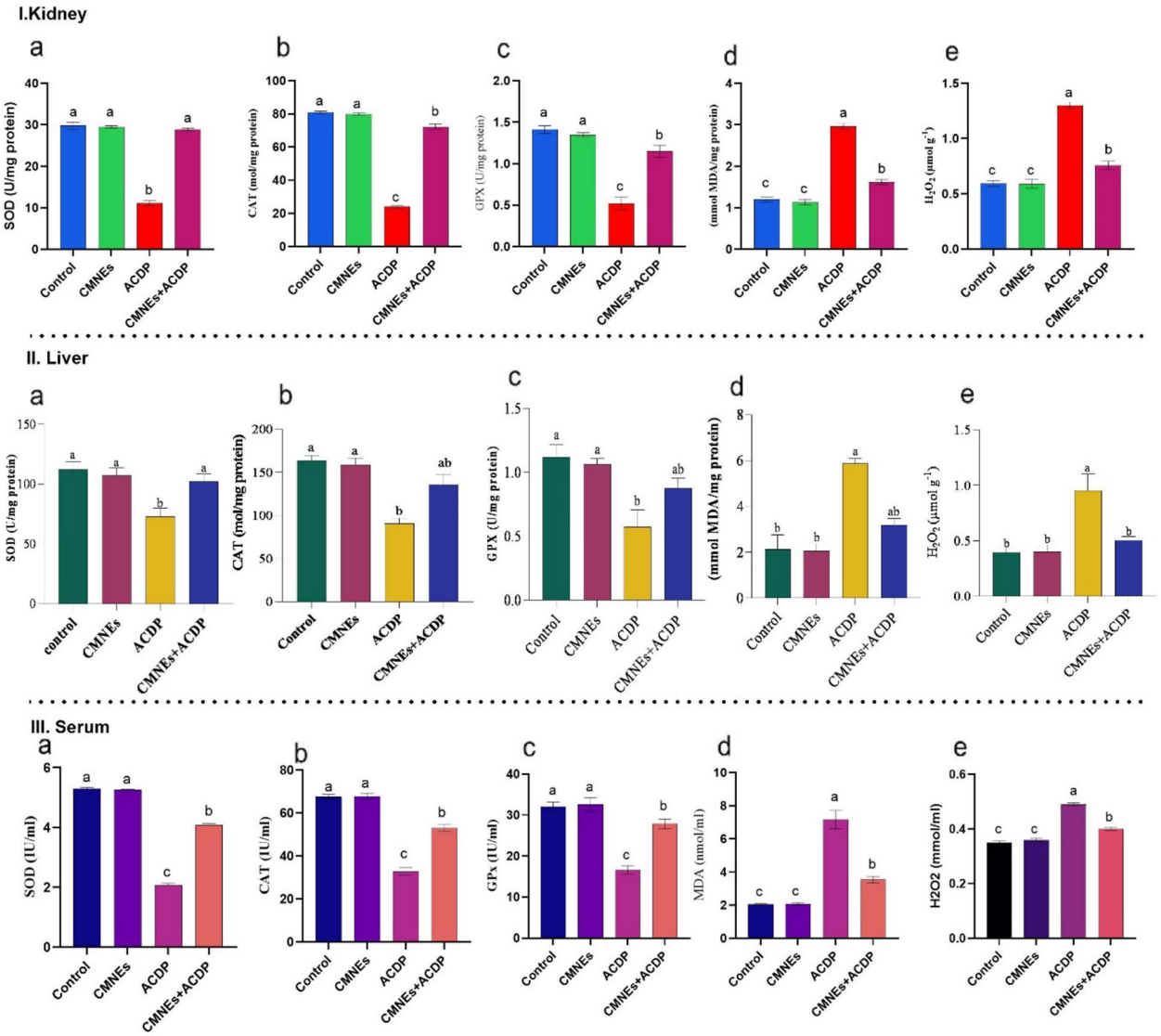

Fig. 3 Effects of cinnamon nanoemulsion (CMNEs; G II) and acetamiprid (ACPD; G III) alone and together (G IV) on oxidative stress and antioxidant markers on the kidney (I), liver(II) and serum (III) of rats ($n = 10$) compared with control (G I). SOD = superoxide dismutase (**a**); CAT = catalase (**b**); GPx = glutathione peroxides (**c**); H_2O_2 = hydrogen peroxide (**e**); MDA = malondialdehyde (**d**); ALT = alanine aminotransferase (**f**); AST = aspartate amino transaminase (**g**); ALP = alkaline phosphatase (**h**). The letters represent the statistically significant differences at ($p < 0.05$) for comparison between all groups, followed by Tukey's post hoc test

interpreted as acetamiprid treatment, which indicates the potentially hazardous effects of this chemical [7]. Moreover, rats treated with ACDP at 30 mg/kg orally for 35 days had lower BWG [61]. In addition, a discernible decrease in the body weight of mice was marked in the ACDP-treated group compared to the control group [62]. This effect is likely due to the toxic impact of acetamiprid on physiological functions, which may include disruption of normal metabolic processes or organ function, leading to an overall decrease in the health and growth rate of the animals. The reduced body weight gain is a standard indicator of systemic toxicity in such exposure scenarios [63].

On the other hand, the body weight was recovered after the coadministration of CMNEs at 2 mg/kg BW. This result was congruent with the findings of Huang and Chen [64], who reported that CMNEs boosted the BWG of rats, possibly due to their regulatory effect in enhancing antioxidant activity. As a result, a disruption in food intake might be responsible for the decrease in body weight growth observed following ACDP administration. Our result was also supported by [64], who revealed

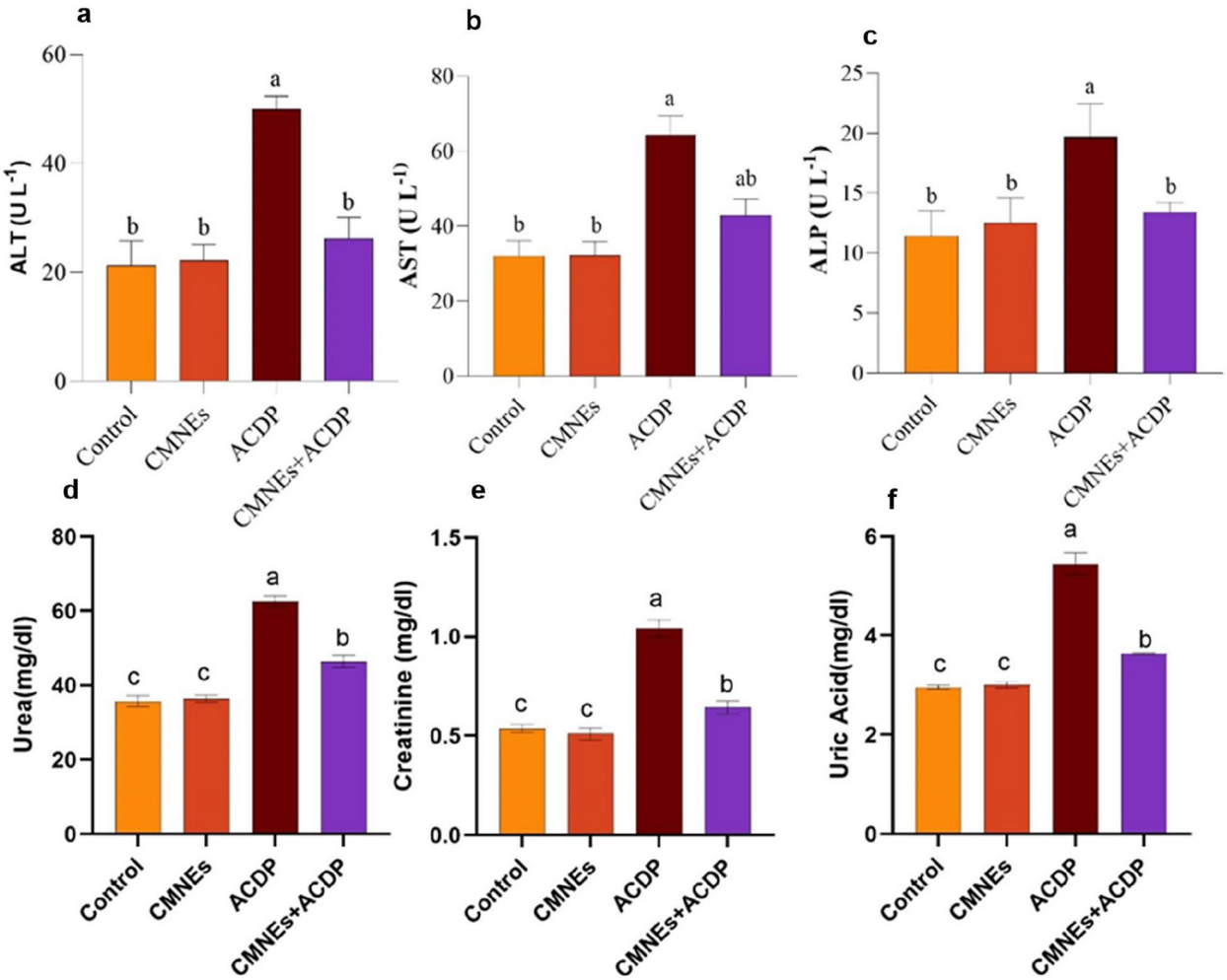

Fig. 4 Effects of cinnamon nanoemulsion (CMNEs; G II) and acetamiprid (ACPD; G III) alone and together (G IV) on hepatic and renal function markers ($n = 10$) compared with control (G I). ALT= (**a**); AST (**b**); ALP (**c**); Urea (**d**; Creatinine (**e**); Uric Acid (**f**); The different letters represent the statistically significant differences at ($p < 0.05$) for comparison between all groups followed by Tukey's post hoc test

that the cinnamon nanoemulsion was effective in lowering body weight loss in diabetic rats and showed that the effectiveness of the nanoemulsion absorption.

Hematological findings demonstrated a remarkable decline in RBC counts, Hb concentration, HC, and PLT levels in the ACDP-treated group relative to the control group. The lysis of RBC brought on by oxidative damage to the cell membranes generated by ROS might cause a decrease in both RBC and Hb [65]. Moreover, this decrease could be produced by a failure in the generation of red blood cells or by an increase in the destruction of erythrocytes. This might be why the anemia and decreased Hb levels are linked to these pesticides [66]. Our findings agreed with Singh et al. [66], who confirmed that male and female mice treated with ACDP had lower RBC counts and hemoglobin concentrations in their blood. Notably, higher WBC and lymphocyte counts following ACDP treatment mirrored an active immunological response in the animals, presumably due to pesticide-induced necrosis and tissue damage [67]. The rise in WBC counts may be a pathogenic reaction. These cells substantially impact during infestation by inducing the immune system and hemopoietic organs to create antibodies in response to the stress caused by ACDP [68]. The increase in WBC counts in rats receiving acetamiprid was verified by Celik et al. [69].

The investigation into oxidative stress markers reveals significant insights into the underlying mechanisms of acetamiprid-induced toxicity and the protective role of cinnamon nanoemulsion. Acetamiprid, a neonicotinoid pesticide, has been documented to induce oxidative stress by generating reactive oxygen species (ROS) in hepatic and renal tissues, leading to elevated levels of malondialdehyde (MDA), a primary marker of lipid

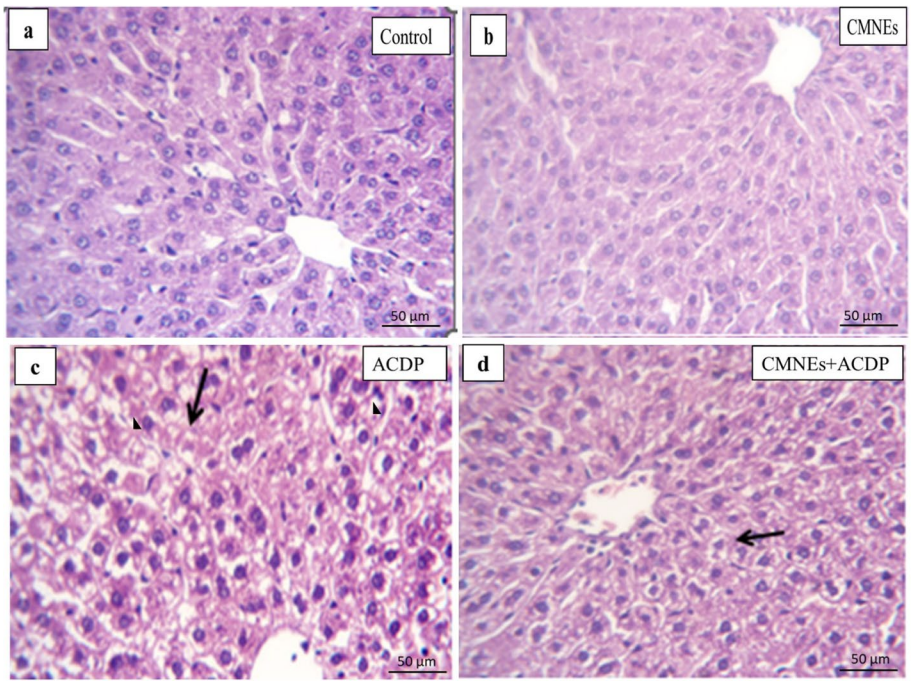

Fig. 5 Photomicrograph of H&E-stained sections from the liver showing degenerative changes, necrotic changes, congested blood vessels, and round cells infiltration. **a** normal central vein and hepatic parenchyma. **b** normal cytoarchitectures of hepatic parenchyma. **c** severe degenerated and necrotic hepatocytes (arrow) with congested hepatic blood vessels (arrowhead) in the rat's group treated with ACDP (arrow). **d** normal hepatic cords with degenerative changes within some hepatocytes (arrow)

peroxidation and cellular damage. This increase in MDA signifies enhanced lipid peroxidation, a direct consequence of oxidative stress and a critical factor in the pathogenesis of organ damage [70]. Furthermore, the overproduction of ROS in the liver precipitated by the ACDP metabolism by hepatic enzymes leads to oxidative damage such as lipid peroxidation, protein breakdown, and DNA damage [71]. Another study claimed that ACDP raised the level of MDA, signifying that lipid peroxidation had been induced. This could have resulted in the loss of membrane structure and function [61]. Antioxidant enzymes like SOD, CAT, and GPx protect cells from oxidative stress by converting superoxide radicals into less harmful substances like water and oxygen [72]. GPx safeguards cellular molecules by reducing hydroperoxides to water, while MDA, a lipid peroxidation product, indicates oxidative damage to cells [73]. In agreement with our research, ACDP-treated rats had significantly lower CAT, SOD, and GPx activities, as well as higher levels of MDA and H2O2. ACDP produces oxidative stress by generating hydroxyl radicals, superoxide anions, nitric oxide, and hydrogen peroxide, contributing to lipid peroxidation [74, 75]. In addition, Ghazanfari et al. [76] reported that the presence of oxidative stress in hepatic cells was suggested by enhanced lipid peroxidation, oxidation of thiol groups, and a decrease in SOD activity in hepatic tissues of ACDP-treated groups.

Conversely, cinnamon nanoemulsion, rich in antioxidant compounds such as phenolic acids and flavonoids, has demonstrated a potent capacity to scavenge these harmful ROS. Enzymatic antioxidants like superoxide dismutase (SOD), catalase (CAT), and glutathione peroxidase (GPx) play crucial roles in the body's defense mechanism against oxidative stress. SOD catalyzes the dismutation of the superoxide anion into hydrogen peroxide, which is then further decomposed to water and oxygen by CAT and GPx, thus mitigating cellular oxidative damage [77]. Likewise, the level of CAT, SOD, and GPx activities decreased with ACDP-treated groups [78].

In contrast, CMNEs stopped the rise in MDA and H2O2 levels as well as the reductions in CAT, SOD, and GPx activity. Our results aligned with a recent study conducted by Berktas and Peker [27], exposing that coadministration of cinnamon along with malathion provoked higher CAT concentration compared to the administration of malathion alone. Additionally, the cotreatment of cinnamon with diclofenac sodium or cinnamon alone lessened the MDA level and enhanced the level of SOD and CAT compared with diclofenac sodium alone [79]. The study found that a high-dose nanoemulsion, rich in phenolic acids and flavonoids, significantly reduced

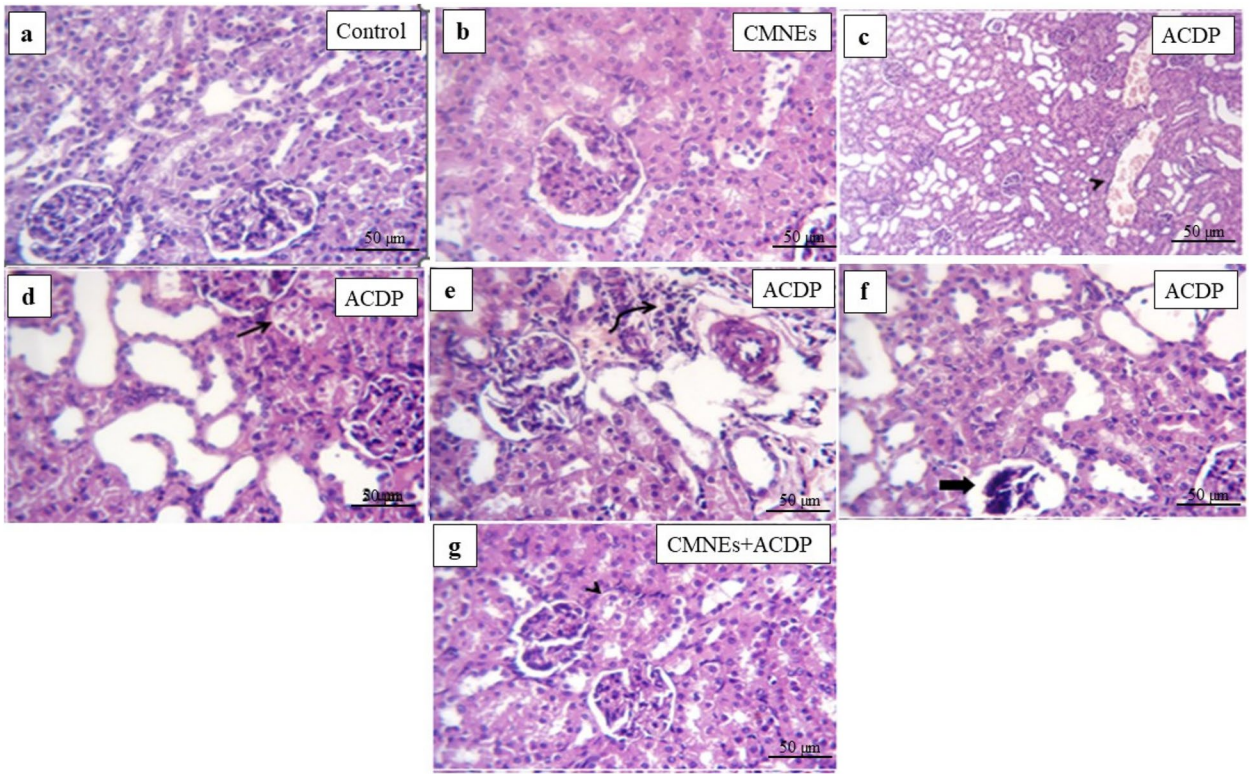

Fig. 6 Photomicrograph of H&E-stained sections from kidney showing some parameters (Dilated tubular lumina, glomerular shrinkage, degenerative changes, necrotic changes, round cells infiltrations). **a** Normal glomerular architectures (arrow) and surrounding renal tubule (arrowhead) are in control. **b** normal architectures of the glomerular and surrounding tubules of the kidney. **c**, **d**, **e**, **f** Severe congestion of the renal blood vessels (arrowhead), dilatation of most tubules, perivascular round cells infiltration (curved arrow), Marked hydropic degeneration and necrosis of tubular epithelium (arrow) and atrophy of some glomerular tufts (thick arrow). **g** normal renal tubules and glomerular structures with some degenerative changes in the renal epithelium (arrowhead)

MDA levels, indicating its potent antioxidant activity in decreasing oxidative damage [80]. The protective effects of cinnamon nanoemulsion in mitigating acetamiprid-induced toxicity can be attributed to its antioxidant properties, which enhance the activity of critical antioxidant enzymes and reduce markers of oxidative stress like MDA. These results provide a promising basis for further research into the use of plant extract nanoemulsions in protecting against chemical-induced organ damage [81].

ACDP may have both inflammatory and immunosuppressive effects [82]. This hypothesis is consistent with our observations that ACDP leads to detrimental biochemical impact on the liver, as seen by noticeably elevated blood levels of ALT, AST, and ALP, and that CMNEs inhibit these elevations. The damage in the liver of rats administrated with ACDP may be due to heightened permeability of the cell membrane [83]. Consequently, transaminases are released into the bloodstream, causing hepatocyte injury and numerous coagulation factors [84], and their inhibitors cannot be adequately synthesized, constricting blood arteries. These findings are consistent with those by Khovarnagh and Seyedalipour [14], reporting that ALT, AST, and ALP levels were elevated in serum after ACDP administration compared with control.

Moreover, the administration of cinnamon decoction remarkably curtailed AST, ALT, and ALP levels compared to restraint-stressed rats [85]. In addition, coadministration of cinnamon plus acetaminophen treatment significantly reduced AST, ALT, and ALP activities compared with acetaminophen alone [86]. Likewise, cotreatment with cinnamon oil plus deltamethrin group reduced the increased AST, ALT, and ALP activities [87].

The most noticeable histological variation showed up as diffuse patches of hydropic degeneration and necrotic hepatocyte evidence. On the contrary, in the kidney, severe congestion of the renal blood vessels, perivascular round cells infiltration, marked hydropic degeneration and necrosis of tubular epithelium, and atrophy of some glomerular tufts was recognized, which results in fluid leakage from the vascular compartment into the interstitium [88]. Our data aligns with research by Mondal

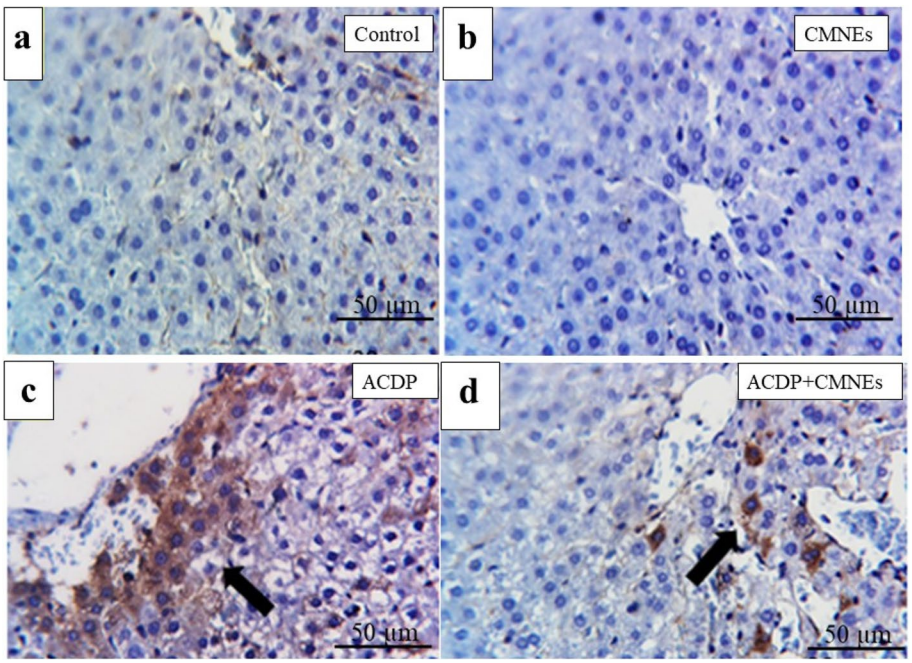

Fig. 7 Photomicrographs of Cox2 immunohistochemistry staining in hepatic sections showing (**a**, **b**) negative expressions of Cox2 in control (GI) and CMNEs, respectively. **c** diffuse immunoexpression of Cox2 in ACDP-treated rats (arrow). **d** few numbers of immunostained cells by anti-Cox2 in ACDP + CMNEs treated rats (arrow). IHC counterstaining with Mayer's hematoxylin. Scale bar 20 µm

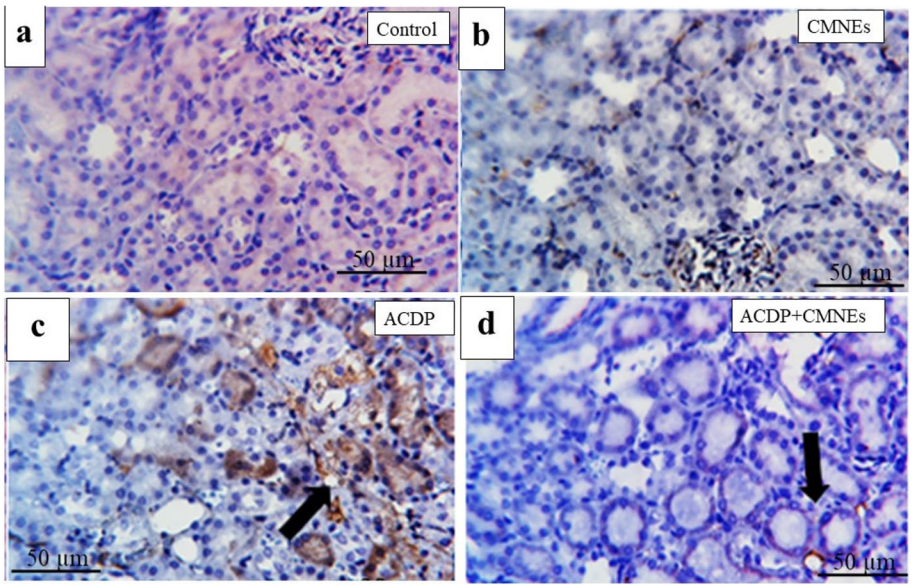

Fig. 8 Photomicrographs of Cox2 immunohistochemistry staining in kidney showing (**a**, **b**) negative expressions of Cox2 in control and CMNEs, respectively. **c** large number of immunoexpressed cells with anti-Cox2 in ACDP-treated rats (arrow). **d** few numbers of immunostained cells by anti-Cox2 in ACDP + CMNEs treated rats (arrow). IHC counterstaining with Mayer's hematoxylin. Scale bar 20 µm

et al. [89] that reported enlargement and petechial hemorrhages in the liver of rats exposed to ACDP. Moreover, ACDP may induce hepatocellular necrosis, fast hepatic architectural disorganization, sinusoidal structure disintegration, and blood pooling in the liver through these processes [90]. Furthermore, tubule deterioration and desquamation of the lining epithelium were discovered by Arıcan et al. [62] in ACDP-treated kidney rats.

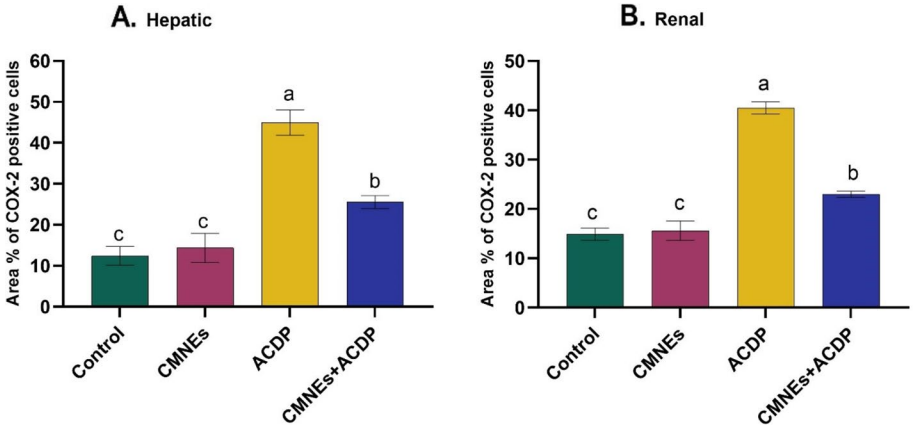

Fig. 9 Area % of Cox-2 positive brown stained cells. In hepatic (**A**) and renal (**B**). All the values were expressed as mean ± SEM. Different small letters indicate significance at $P < 0.05$

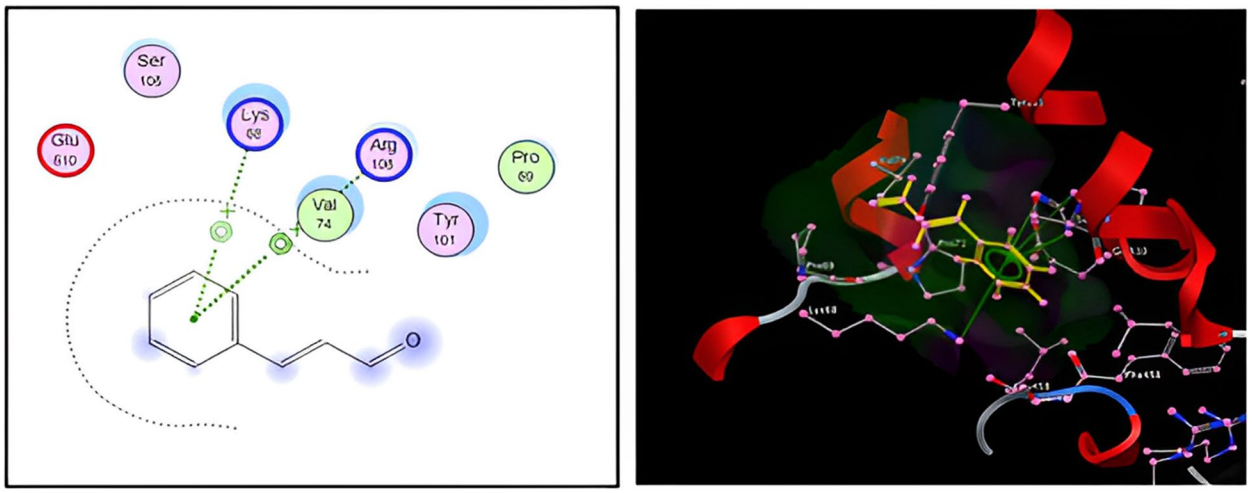

Fig. 10 Docking view of binding interactions of major CMNEs (Cinnamaldehyde) constituent as a ligand with COX-2 as a receptor. Left: two-dimensional interaction diagram of constitute–receptor complexes. Right: the 3D complex structure and ligand bonds are depicted by yellow lines

Additionally, in kidney rats treated with ACDP, Most tubules had coagulative necrosis in the lining epithelium and severe congestion in the cortical blood vessels [91]. Likewise, in ACDP-treated rats, tubular cells were wholly lysed, leaving the reticular framework, and there were degenerative and necrotic alterations in the kidney's proximal and distal convoluted tubules [89].

Our findings proved that CMNEs may have had an ameliorative effect. All previously histological changes were ameliorated when CMNEs and ACDP were administered together, and all acetamiprid-induced toxic effects were modulated to within normal limits. Its antioxidant capabilities might be responsible for this protective function [87]. The investigation's histopathological findings in the ACDP + CMNEs group improved, which was in line with the advancement of biochemical data. Compared to the ACDP group alone, there was a notable decline in the histological changes in this group, and the bulk of the liver and kidney tissue displayed essentially the same structure. Our results agreed with Kardan et al. [92], documenting that CMNEs might speed up healing due to escalated cellular infiltration in rats.

Moreover, CMNEs diminished the adverse effects of deltamethrin absorption and prevented its damaging immune system effects [87]. Furthermore, cinnamon ameliorated cypermethrin-induced histological alterations in the livers of rats [23]. Likewise, the authors in [93] argued that cinnamon protected the liver from the

fatty alterations brought on by cholesterol in rats. An analogous investigation revealed that administering cinnamon extract ameliorated the histological alterations between rats given paracetamol [21]. Additionally, cinnamon has anti-inflammatory and antidiabetic properties and potent biological actions against germs and fungi. It has been used as an anti-inflammatory and anticancer medication. The activity is due to eugenol, trans-cinnamaldehyde, linalool, and other bioactive components [94].

COX-2 is a crucial enzyme that has a role in the pathogenesis of hepatonephrotoxicity. It is commonly acknowledged that it can trigger inflammatory processes linked to many liver illnesses. Xanthine Oxidase speeds up the conversion of hypoxanthine to xanthine and xanthine to uric acid. H_2O_2 and ROS, which are byproducts of this process, play a significant role in the etiology of tissue damage [95]. Our assessments of biochemistry and histology were confirmed by the COX-2 IHC results, which did not expose any cytoplasmic expressions of COX-2 within hepatic and renal tubular cells in control and CMNEs-treated rats. In ACDP-treated rats, COX-2 was detected in the liver and kidney tissues to varied intensity, while immune expressions appeared in a few cells in the ACDP + CMNEs group. Our results are consistent with previous studies demonstrating that nuclear factor kappa B (NF-B) is involved in the upregulation of COX-2 [96]. In addition, the expression of COX-2 protein was intensified after exposure to DDD and DDE [97].

Moreover, it is hypothesized that COX-2 contributed to inflammation and tumor growth. Additionally, xenobiotics may precipitate COX-2 expression by activating NF-B [98]. Also, Expression of COX-2 is associated with inflammation and is released by an array of proinflammatory stimuli [99]. Interestingly, a diffuse positive cytoplasmic expression of COX-2 illustrates the enormous cytoplasmic immunoreactivity for detecting COX-2 antigen in the livers and kidneys of abamectin-treated rats [100].

Another intriguing finding supporting the immunohistochemistry results is that cinnamon aldehyde discloses a strong binding with the COX-2 enzyme, a key player in the pathogenesis of liver and kidney damage. This may be because cinnamaldehyde can operate as a free radical scavenger, antioxidant, and anti-inflammatory agent [101]. Attaining notable downregulation of COX-2 enzyme expression during oxidative stress could be a critical strategy in regulating liver and kidney destruction [100]. Moreover, trans-cinnamaldehyde treatment uncovered anti-inflammatory actions by downregulating COX-2 expressions compared with methotrexate alone [102]. Furthermore, cinnamaldehyde treatment significantly attenuated inflammation in mesenteric liver injuries by downregulating the expression of inflammation-related COX-2 [103].

Our hematological, biochemical, histological, IHC and molecular docking analysis manifested that CMNEs shielded the kidney and liver from renal-hepatic damage caused by ACDP because of their anti-inflammatory and antioxidant qualities.

Conclusion

Our study underscores the significant risks posed by subchronic exposure to acetamiprid (ACDP), a common neonicotinoid insecticide increasingly detected as a dietary contaminant. The findings from our experimental model reveal that ACDP exposure can lead to substantial toxic effects on the hepatic and renal systems in rats, characterized by decreased activities of key antioxidant enzymes. Moreover, significant increases in liver enzymes and kidney markers injury—alongside marked histopathological damage to liver and kidney tissues highlight the severity of ACDP's detrimental impacts. Importantly, our research demonstrates the therapeutic potential of cinnamon nanoemulsions (CMNEs) in mitigating these adverse effects. The coadministration of CMNEs with ACDP substantially ameliorates the observed oxidative stress and inflammation in the hepatic and renal systems. This protective effect is likely mediated through the upregulation of antioxidant defenses, as evidenced by normalized oxidative stress markers and improved histological outcomes. The molecular interactions between cinnamaldehyde, a key component of CMNEs, and cyclooxygenase 2 (COX-2), further elucidate the mechanistic basis of CMNEs' protective efficacy. These findings reinforce the need for caution in the environmental and dietary exposure to acetamiprid and highlight the promising role of bioactive nanoparticle formulations from medicinal plants in enhancing antioxidant defenses. Applying such nanoparticles could serve as a viable strategy to counteract the oxidative stress and organ toxicity induced by various environmental contaminants. Future research should aim to explore the broader applicational scope of these nanoparticles across different models and setups to harness their therapeutic potential fully.

Supplementary Information

The online version contains supplementary material available at https://doi.org/10.1186/s12917-024-04084-x.

Supplementary Material 1.

Acknowledgements

This research was funded by Princess Nourah bint Abdulrahman University Researchers Supporting Project numbers (PNURSP2024R82), and

(PNURSP2024R82), Princess Nourah bint Abdulrahman University, Riyadh, Saudi Arabia.

Authors' contributions
All the authors have contributed to preparing this review paper starting from the conception or design of the work (A.A., S.A., L.A.A.), data acquisition (A.H., M.S.), and analysis (A.A., S.I., S.M.S.), and interpretation of data (M.M.) to drafting and reviewing manuscript (A.A., A.E.).

Funding
This research was funded by Princess Nourah bint Abdulrahman University Researchers Supporting Project numbers (PNURSP2024R82), and (PNURSP2024R82), Princess Nourah bint Abdulrahman University, Riyadh, Saudi Arabia.

Availability of data and materials
No datasets were generated or analysed during the current study.

Declarations

Ethics approval and consent to participate
The animal ethics committee of Zagazig University's Faculty of Agriculture in Egypt reviewed and approved the animal study. Ethical code number ZU-IACUC/2/F/132/2023.

Consent for publication
Not applicable.

Competing interests
The authors declare no competing interests.

Author details
[1]Plant Protection Department, Faculty of Agriculture, Zagazig University, Zagazig 44511, Egypt. [2]Animal Production Department, Faculty of Agriculture, Zagazig University, Zagazig 44511, Egypt. [3]Stored Product Pests Research Department, Plant Protection Research Institute, Agricultural Research Center, Sakha, Kafr El-Sheikh 33717, Egypt. [4]Department of Biochemistry, Faculty of Agriculture, Zagazig University, Zagazig 44511, Egypt. [5]Department of Biology, College of Science, Princess Nourah Bint Abdulrahman University, P.O. Box 84428, Riyadh 11671, Saudi Arabia. [6]Physiology Department, Faculty of Veterinary Medicine, kafrelsheikh University, kafrelsheikh 33516, Egypt. [7]Department of Economic Entomology and Pesticides, Faculty of Agriculture, Cairo University, Giza 12613, Egypt. [8]Department of Science and Technology, University College-Ranyah, Taif University, B.O. Box 11099, Taif 21944, Saudi Arabia.

Received: 10 January 2024 Accepted: 16 May 2024
Published online: 12 June 2024

References

1. Speck-Planche A, Kleandrova VV, Scotti MT. Fragment-based approach for the in silico discovery of multi-target insecticides. Chemometr Intell Lab Syst. 2012;111:39–45.
2. Devan RS, Mishra A, Prabu P, Mandal T, Panchapakesan S. Sub-chronic oral toxicity of acetamiprid in Wistar rats. Toxicol Environ Chem. 2015;97:1236–52.
3. Sanyal AJ, Boyer T, Garcia–Tsao G, Regenstein F, Rossaro L, Appenrodt B, Blei A, Gülberg V, Sigal S, Teuber P. A randomized, prospective, double-blind, placebo-controlled trial of terlipressin for type 1 hepatorenal syndrome. Gastroenterology. 2008;134:1360–8.
4. Su Y, Ren X, Hu H, Song X, Ma X, Wang D, Yao Y, Ma Y, Cui J. Sublethal effects of imidacloprid and clothianidin on the biological traits of predatory lacewing Chrysopa pallens (Rambur)(Neuroptera: Chrysopidae). Crop Prot. 2023;163:106117.
5. Hamadache M, Benkortbi O, Hanini S, Amrane A, Khaouane L, Moussa CS. A quantitative structure activity relationship for acute oral toxicity of pesticides on rats: validation, domain of application and prediction. J Hazard Mater. 2016;303:28–40.
6. Hendawi MY, Alam RT, Abdellatief SA. Ameliorative effect of flaxseed oil against thiacloprid-induced toxicity in rats: hematological biochemical and histopathological study Environ Sci Pollut Res. 23(12). 2016;11855–63. https://doi.org/10.1007/s11356-016-6376-z.
7. Sevim Ç, Akpınar E, Aksu EH, Ömür AD, Yıldırım S, Kara M, Bolat İ, Tsatsakis A, Mesnage R, Golokhvast KS. Reproductive effects of S. boulardii on Sub-chronic Acetamiprid and Imidacloprid Toxicity in male rats. Toxics. 2023;11:170.
8. Brunet JL, Badiou A, Belzunces LP. In vivo metabolic fate of [14 C]-acetamiprid in six biological compartments of the honeybee, Apis mellifera L. Pest Manage Science: Former Pesticide Sci. 2005;61:742–8.
9. Goulson D. An overview of the environmental risks posed by neonicotinoid insecticides. J Appl Ecol. 2013;50:977–87.
10. Ford KA, Casida JE. Unique and common metabolites of thiamethoxam, clothianidin, and dinotefuran in mice. Chem Res Toxicol. 2006;19:1549–56.
11. Chakroun S, Ezzi L, Grissa I, Kerkeni E, Neffati F, Bhouri R, Sallem A, Najjar MF, Hassine M, Mehdi M. Hematological, biochemical, and toxicopathic effects of subchronic acetamiprid toxicity in Wistar rats. Environ Sci Pollut Res. 2016;23:25191–9.
12. Toghan R, Amin YA, Ali RA, Fouad SS, Ahmed MA-EB, Saleh SM. Protective effects of folic acid against reproductive, hematological, hepatic, and renal toxicity induced by Acetamiprid in male albino rats. Toxicology. 2022;469:153115.
13. Yan S, Meng Z, Tian S, Teng M, Yan J, Jia M, Li R, Zhou Z, Zhu W. Neonicotinoid insecticides exposure cause amino acid metabolism disorders, lipid accumulation and oxidative stress in ICR mice. Chemosphere. 2020;246:125661.
14. Khovarnagh N, Seyedalipour B. Antioxidant, histopathological and biochemical outcomes of short-term exposure to acetamiprid in liver and brain of rat: the protective role of N-acetylcysteine and S-methylcysteine. Saudi Pharm J. 2021;29:280–9.
15. Bagri P, Jain S. Assessment of acetamiprid-induced genotoxic effects in bone marrow cells of Swiss albino male mice. Drug Chem Toxicol. 2019;42:357–63.
16. Osman KA, El-Din EME, Ahmed NS, Ayman S. Effect of N-acetylcysteine on attenuation of chlropyrifos and its methyl analogue toxicity in male rats. Toxicology. 2021;461:152904.
17. Gokhan T, Smith P, Lee M. GUSUM: graph-based unsupervised summarization using sentence features scoring and sentence-BERT. In: Proceedings of TextGraphs-16: graph-based methods for natural language processing. 2022. p. 44–53.
18. Eidi A, Mortazavi P, Bazargan M, Zaringhalam J. Hepatoprotective activity of cinnamon ethanolic extract against CCl4-induced liver injury in rats. EXCLI J. 2012;11:495.
19. Rao PV, Gan SH. Cinnamon: a multifaceted medicinal plant. Evid Based Complement Altern Med. 2014;2014:642942.
20. Herdwiani W, Soemardji A, Tan M. A review of cinnamon as a potent anticancer drug. Asian J Pharm Clin Res. 2016:8–13.
21. Elkomy A, Aboubakr M, Soliman A, Abdeen A, Abdelkader A, Hekal H. Paracetamol induced hepatic toxicity and amelioration by cinnamon in rats. Int J Pharmacol Toxicol. 2016;4:187.
22. Moselhy SS, Ali HK. Hepatoprotective effect of cinnamon extracts against carbon tetrachloride induced oxidative stress and liver injury in rats. Biol Res. 2009;42:93–8.
23. Sakr SA, Hashem AM, Nofal AE, El-shaer NH. Protective effect of cinnamon aqueous extract on cypermethrin-induced hepatotoxicity in albino rats. World J Pharm Sci. 2017:119–28.
24. Refat MS, Hamza RZ, Adam AMA, Saad HA, Gobouri AA, Azab E, Al-Salmi FA, Altalhi TA, Khojah E, Gaber A. Antioxidant, antigenotoxic, and hepatic ameliorative effects of quercetin/zinc complex on cadmium-induced hepatotoxicity and alterations in hepatic tissue structure. Coatings. 2021;11:501.
25. Gupta A, Eral HB, Hatton TA, Doyle PS. Nanoemulsions: formation, properties and applications. Soft Matter. 2016;12:2826–41.
26. Sheth T, Seshadri S, Prileszky T, Helgeson ME. Multiple nanoemulsions. Nat Reviews Mater. 2020;5:214–28.
27. Berktas OA, Peker EGG. The investigation of the protective effect of cinnamon water extract and vitamin E on malathion-induced oxidative damage in rats. Toxicol Res. 2021;10:627–30.

28. Hamouda T, Hayes MM, Cao Z, Tonda R, Johnson K, Wright DC, Brisker J, Baker JR Jr. A novel surfactant nanoemulsion with broad-spectrum sporicidal activity against Bacillus species. J Infect Dis. 1999;180:1939–49.
29. Hashem AS, Awadalla SS, Zayed GM, Maggi F, Benelli G. Pimpinella anisum essential oil nanoemulsions against Tribolium castaneum—insecticidal activity and mode of action. Environ Sci Pollut Res. 2018;25:18802–12.
30. Stenzel YP, Winter M, Nowak S. Evaluation of different plasma conditions and resolutions for understanding elemental organophosphorus analysis via GC-ICP-SF-MS. J Anal at Spectrom. 2018;33:1041–8.
31. Li Y, Kong W, Li M, Liu H, Zhao X, Yang S, Yang M. Litsea cubeba essential oil as the potential natural fumigant: inhibition of aspergillus flavus and AFB1 production in licorice. Ind Crops Prod. 2016;80:186–93.
32. Adams RP. Identification of essential oil components by gas chromatography/quadrupole mass spectrometry. Carol Stream: Allured Publishing Corporation; 2001.
33. Sohrabi R, Pazgoohan N, Seresht HR, Amin B. Repeated systemic administration of the cinnamon essential oil possesses anti-anxiety and anti-depressant activities in mice. Iran J Basic Med Sci. 2017;20:708.
34. Murakami M, Niwa H, Kushikata T, Watanabe H, Hirota K, Ono K, Ohba T. Inhalation anesthesia is preferable for recording rat cardiac function using an electrocardiogram. Biol Pharm Bull. 2014;37:834–9.
35. Nishikimi M, Rao NA, Yagi K. The occurrence of superoxide anion in the reaction of reduced phenazine methosulfate and molecular oxygen. Biochem Biophys Res Commun. 1972;46:849–54.
36. Aebi H. [13] Catalase in vitro. In methods in enzymology, vol. 105. Academic press; 1984. p. 121–126.
37. Paglia DE, Valentine WN. Studies on the quantitative and qualitative characterization of erythrocyte glutathione peroxidase. J Lab Clin Med. 1967;70:158–69.
38. Lowry OH, Rosebrough NJ, Farr AL, Randall RJ. Protein measurement with the Folin phenol reagent. J biol Chem. 1951;193:265–75.
39. Ohkawa H, Ohishi N, Yagi K. Assay for lipid peroxides in animal tissues by thiobarbituric acid reaction. Anal Biochem. 1979;95:351–8.
40. Pick E, Keisari Y. A simple colorimetric method for the measurement of hydrogen peroxide produced by cells in culture. J Immunol Methods. 1980;38:161–70.
41. Reitman S, Frankel S. A colorimetric method for the determination of serum glutamic oxalacetic and glutamic pyruvic transaminases. Am J Clin Pathol. 1957;28:56–63.
42. Ellis G, Belfield A, Goldberg DM. Colorimetric determination of serum acid phosphatase activity using adenosine 3′-monophosphate as substrate. J Clin Pathol. 1971;24:493–500.
43. Spencer L, Bancroft J, Bancroft J, Gamble M. Tissue processing. Bancroft's theory and practice of histological techniques. 7nd ed. Amsterdam: Elsevier Health Sciences; 2012. p. 105–23.
44. Hsu S-M, Raine L, Fanger H. Use of avidin-biotin-peroxidase complex (ABC) in immunoperoxidase techniques: a comparison between ABC and unlabeled antibody (PAP) procedures. J Histochem Cytochemistry. 1981;29:577–80.
45. Hewitt SM, Baskin DG, Frevert CW, Stahl WL, Rosa-Molinar E. Controls for immunohistochemistry: the Histochemical Society's standards of practice for validation of immunohistochemical assays. J Histochem Cytochemistry. 2014;62:693–7.
46. Devi ID. Comparative binding mode of organophosphates, pyrethroids against modelled structures of acetylcholinesterase and alpha amylase in Blattella germanica. J Entomol Zool Stud. 2015;3:233–8.
47. Zhang N, Liu J, Chen SN, Huang LH, Feng QL, Zheng SC. Expression profiles of glutathione S-transferase superfamily in Spodoptera litura tolerated to sublethal doses of chlorpyrifos. Insect Sci. 2016;23:675–87.
48. Khatib I, Rychter P, Falfushynska H. Pesticide pollution: detrimental outcomes and possible mechanisms of fish exposure to common organophosphates and triazines. J Xenobiotics. 2022;12:236–65.
49. Sharma N, Bansal M, Visht S, Sharma P, Kulkarni G. Nanoemulsion: a new concept of delivery system. Chronicles Young Scientists. 2010;1:2–6.
50. Gorain B, Choudhury H, Nair AB, Dubey SK, Kesharwani P. Theranostic application of nanoemulsions in chemotherapy. Drug Discovery Today. 2020;25:1174–88.
51. Patakangas J. Investigation of electrolyte materials and measurement techniques for nanocomposite fuel cells. 2014.
52. Shi B, Wang Z, Wen H. Research on the strengths of electrostatic and Van Der Waals interactions in ionic liquids. J Mol Liq. 2017;241:486–8.
53. Hoeller S, Sperger A, Valenta C. Lecithin based nanoemulsions: a comparative study of the influence of non-ionic surfactants and the cationic phytosphingosine on physicochemical behaviour and skin permeation. Int J Pharm. 2009;370:181–6.
54. Arancibia C, Navarro-Lisboa R, Zúñiga RN, Matiacevich S. Application of CMC as thickener on nanoemulsions based on olive oil: Physical properties and stability. Int J Polym Sci. 2016
55. Farag MA, Khaled SE, El Gingeehy Z, Shamma SN, Zayed A. Comparative metabolite profiling and fingerprinting of medicinal cinnamon bark and its commercial preparations via a multiplex approach of GC–MS, UV, and NMR techniques. Metabolites. 2022;12:614.
56. Wang Y, Ocariz J, Hammersand J, MacDonald E, Bartczak A, Kero F, Young VY, Williams KR. Determination of cinnamaldehyde in cinnamon by SPME–GC–MS. an instrumental analysis experiment. J Chem Educ. 2008;85:957.
57. Suryanti V, Wibowo FR, Khotijah S, Andalucki N. Antioxidant activities of cinnamaldehyde derivatives. In IOP conference series: Materials science and engineering, vol. 333. IOP Publishing; 2018. p. 012077.
58. Kuttithodi AM, Narayanankutty A, Visakh NU, Job JT, Pathrose B, Olatunji OJ, Alfarhan A, Ramesh V. Chemical composition of the Cinnamomum malabatrum Leaf Essential Oil and analysis of its antioxidant, enzyme inhibitory and antibacterial activities. Antibiotics. 2023;12:940.
59. Perry NB, Anderson RE, Brennan NJ, Douglas MH, Heaney AJ, McGimpsey JA, Smallfield BM. Essential oils from Dalmatian sage (Salvia officinalis L.): variations among individuals, plant parts, seasons, and sites. J Agric Food Chem. 1999;47:2048–54.
60. Manisalidis I, Stavropoulou E, Stavropoulos A, Bezirtzoglou E. Environmental and health impacts of air pollution: a review. Front Public Health. 2020;8:14.
61. Zhang JJ, Yi W, Xiang HY, Li MX, Li WH, Wang XZ, Zhang JH. Oxidative stress: role in acetamiprid-induced impairment of the male mice reproductive system. Agric Sci China. 2011;10:786–96.
62. Arıcan EY, Gökçeoğlu Kayalı D, Ulus Karaca B, Boran T, Öztürk N, Okyar A, Ercan F, Özhan G. Reproductive effects of subchronic exposure to acetamiprid in male rats. Sci Rep. 2020;10:8985.
63. Phogat A, Singh J, Kumar V, Malik V. Toxicity of the acetamiprid insecticide for mammals: A review. Environ Chem Lett. 2022;1–26.
64. Huang Y-C, Chen B-H. A comparative study on improving streptozotocin-induced type 2 diabetes in rats by hydrosol, extract and nanoemulsion prepared from cinnamon leaves. Antioxidants. 2022;12:29.
65. Dhaliwal G, Cornett PA, Tierney LM Jr. Hemolytic anemia. Am Fam Phys. 2004;69:2599–607.
66. Singh TB, Mukhopadhayay SK, Sar TK, Ganguly S. Acetamiprid induces toxicity in mice under experimental conditions with prominent effect on the hematobiochemical parameters. J Drug Metab Toxicol. 2012;3:134.
67. Meligi NM, Hassan HF. Protective effects of Eruca sativa (rocket) on abamectin insecticide toxicity in male albino rats. Environ Sci Pollut Res. 2017;24:9702–12.
68. Lebelo S, Saunders D, Crawford T. Observations on blood viscosity in striped bass, Morone saxatilis (Walbaum) associated with fish hatchery conditions. Trans Kans Acad Sci. 2001;104:183–94.
69. Celik B, Sahin E, Nadir A, Kaptanoglu M. Iatrogenic pneumothorax: etiology, incidence and risk factors. Thorac Cardiovasc Surg. 2009;57:286–90.
70. Amiri M. Oxidative stress and free radicals in liver and kidney diseases; an updated short-review. J Nephropathol. 2018;7(3).
71. Selvakumar K, Bavithra S, Suganthi M, Benson CS, Elumalai P, Arunkumar R, Krishnamoorthy G, Venkataraman P, Arunakaran J. Protective role of quercetin on PCBs-induced oxidative stress and apoptosis in hippocampus of adult rats. Neurochem Res. 2012;37:708–21.
72. Scassellati C, Galoforo AC, Bonvicini C, Esposito C, Ricevuti G. Ozone: a natural bioactive molecule with antioxidant property as potential new strategy in aging and in neurodegenerative disorders. Ageing Res Rev. 2020;63:101138.
73. Rao AK, Shaha C. Role of glutathione S-transferases in oxidative stress–induced male germ cell apoptosis. Free Radic Biol Med. 2000;29:1015–27.

74. Eltoweissy MY, El-Din EME, Osman KA. Acetamiprid induced oxidative stress and genotoxicity in male albino rats: attenuation by ambroxol. 2022.
75. Faria JCT, Ribeiro-Kumara C, Delarmelina WM, Namorato FA, Momolli DR, José AC, Konzen ER, de Carvalho D, Brondani GE. Evaluation of total protein, peroxidase, and nutrients measured by pXRF for the determination of tissue rejuvenation/reinvigoration of Eucalyptus microcorys. J Forest Res. 2023;34:1563–76.
76. Ghazanfari A, Soodi M, Omidi A. Quercetin ameliorates acetamiprid-inducedhepatotoxicity and oxidative stress. Physiol Pharmacol. 2021;25:154–61.
77. Erdemli ME, Zayman E, Erdemli Z, Gul M, Gul S. Gozukara Bag, protective effects of melatonin and vitamin E in acetamiprid-induced nephrotoxicity. Environ Sci Pollut Res. 2020;27:9202–13.
78. Hathout HM, Sobhy HM, Abou-Ghanima S, El-Garawani IM. Ameliorative role of ascorbic acid on the oxidative stress and genotoxicity induced by acetamiprid in Nile tilapia (Oreochromis niloticus). Environ Sci Pollut Res. 2021;28:55089–101.
79. Elshopakey GE, Elazab ST. Cinnamon aqueous extract attenuates diclofenac sodium and oxytetracycline mediated hepato-renal toxicity and modulates oxidative stress, cell apoptosis, and inflammation in male albino rats. Veterinary Sci. 2021;8:9.
80. Wang YC, Wang V, Chen BH. Analysis of bioactive compounds in cinnamon leaves and preparation of nanoemulsion and byproducts for improving Parkinson's disease in rats. Front Nutr. 2023;10:1229192.
81. Huyut Z, Beydemir Ş, Gülçin İ. Antioxidant and antiradical properties of selected flavonoids and phenolic compounds. Biochem Res Int. 2017;2017:7616791.
82. Shahin M. Hepatoprotective effect of ginseng, green tea, cinnamon their combination against acetamiprid-induced oxidative stress in rats. Asian J Biol. 2018;5:1–13.
83. González-Recio I, Simón J, Goikoetxea-Usandizaga N, Serrano-Maciá M, Mercado-Gómez M, Rodríguez-Agudo R, Lachiondo-Ortega S, Gil-Pitarch C, Fernández-Rodríguez C, Castellana D. Restoring cellular magnesium balance through cyclin M4 protects against acetaminophen-induced liver damage. Nat Commun. 2022;13:6816.
84. Sathiavelu J, Senapathy GJ, Devaraj R, Namasivayam N. Hepatoprotective effect of chrysin on prooxidant-antioxidant status during ethanol-induced toxicity in female albino rats. J Pharm Pharmacol. 2009;61:809–17.
85. Khataibeh M. Cinnamon modulates biochemical alterations in rats loaded with acute restraint stress. J Saudi Chem Soc. 2016;20:S411–4.
86. Hussain S, Ashafaq M, Alshahrani S, Siddiqui R, Ahmed RA, Khuwaja G, Islam F. Cinnamon oil against acetaminophen-induced acute liver toxicity by attenuating inflammation, oxidative stress and apoptosis. Toxicol Rep. 2020;7:1296–304.
87. Ahmed W, Abdel-Azeem N, Ibrahim M, Helmy N, Radi A. The impact of cinnamon oil on hepatorenal toxicity and antioxidant related gene expression induced by deltamethrin in rat. Adv Anim Vet Sci. 2021;9:1071–7.
88. Gao P, Zhu J, Yan Q, Yang K, Zhang J. The amelioration of degraded larch (Larix olgensis) soil depends on the proportion of Aralia elata litter in larch-A. elata agroforestry systems. J Forest Res. 2023;34:1065–76.
89. Mondal S, Ghosh RC, Karnam SS, Purohit K. Toxicopathological changes on Wistar rat after multiple exposures to acetamiprid. Vet World. 2014;7(12).
90. Edinger AL, Thompson CB. Death by design: apoptosis, necrosis and autophagy. Curr Opin Cell Biol. 2004;16:663–9.
91. Noaishi MA, Abd Alhafez H. Hepatotoxicity and nephrotoxicity evaluation after repeated dose of acetamiprid in albino rats. Egypt J Chem Environ Health. 2016;2:439–52.
92. Kardan T, Mohammadi R, Taghavifar S, Cheraghi M, Yahoo A, Mohammadnejad K. Polyethylene glycol–based Nanocerium improves healing responses in Excisional and Incisional Wound models in rats. Int J Low Extrem Wounds. 2021;20:263–71.
93. Iqbal Z, Iqbal K, Mudassar M. Hepatoprotective effect of cinnamon on cholesterol induced fatty changes in Albino rats . Isra Med J. 2015;7(4).
94. Shahid MZ, Saima H, Yasmin A, Nadeem MT, Imran M, Afzaal M. Antioxidant capacity of cinnamon extract for palm oil stability. Lipids Health Dis. 2018;17:1–8.
95. Osukoya OA, Oyinloye BE, Ajiboye BO, Olokode KA, Adeola HA. Nephroprotective and anti-inflammatory potential of aqueous extract from Persea americana seeds against cadmium-induced nephrotoxicity in Wistar rats. Biometals. 2021;34:1141–53.
96. Surh YJ, Chun KS, Cha HH, Han SS, Keum YS, Park KK, Lee SS. Molecular mechanisms underlying chemopreventive activities of anti-inflammatory phytochemicals: down-regulation of COX-2 and iNOS through suppression of NF-κB activation. Mutat Res. 2001;480:243–68.
97. Dominguez-Lopez P, Diaz-Cueto L, Olivares A, Ulloa-Aguirre A, Arechavaleta-Velasco F. Differential effect of DDT, DDE, and DDD on COX-2 expression in the human trophoblast derived HTR-8/SVneo cells. J Biochem Mol Toxicol. 2012;26:454–60.
98. Kumar KS, Wang S-Y. Lucidone inhibits iNOS and COX-2 expression in LPS-induced RAW 264.7 murine macrophage cells via NF-κB and MAPKs signaling pathways. Planta Med. 2009;75:494–500.
99. Loftin CD, Tiano HF, Langenbach R. Phenotypes of the COX-deficient mice indicate physiological and pathophysiological roles for COX-1 and COX-2. Prostaglandins Other Lipid Mediat. 2002;68:177–85.
100. Aioub AA, Abdelnour SA, Shukry M, Saad AM, El-Saadony MT, Chen Z, Elsobki AE. Ameliorating effect of the biological zinc nanoparticles in abamectin induced hepato-renal injury in a rat model: implication of oxidative stress, biochemical markers and COX-2 signaling pathways. Front Pharmacol. 2022;13:947303.
101. Spisni E, Petrocelli G, Imbesi V, Spigarelli R, Azzinnari D, Donati Sarti M, Campieri M, Valerii MC. Antioxidant, anti-inflammatory, and microbial-modulating activities of essential oils: implications in colonic pathophysiology. Int J Mol Sci. 2020;21:4152.
102. El-Tanbouly GS, Abdelrahman RS. Novel anti-arthritic mechanisms of trans-cinnamaldehyde against complete Freund's adjuvant-induced arthritis in mice: involvement of NF-κB/TNF-α and IL-6/IL-23/IL-17 pathways in the immuno-inflammatory responses. Inflammopharmacology. 2022;30:1769–80.
103. Almoiliqy M, Wen J, Qaed E, Sun Y, Lian M, Mousa H, Al-Azab M, Zaky MY, Chen D, Wang L. Protective effects of cinnamaldehyde against mesenteric ischemia-reperfusion-induced lung and liver injuries in rats. Oxid Med Cell Longev. 2020;2020:4196548.

Publisher's Note